Effect of curing systems on polymer–filler interaction, technical properties and fracture mode of carboxylated nitrile rubber

Sunity K. Chakraborty and Sadhan K. De
Rubber Technology Centre, Indian Institute of Technology, Kharagpur 721302, India
(Received 11 August 1982; revised 2 December 1982)

The effects of carbon black on polymer–filler interaction, technical properties and fracture mode of carboxylated nitrile rubber (XNBR) cured by different curing systems have been studied. Technical properties show improvement in all cases with increase of filler loadings. At lower loadings of filler, a marked difference in physical properties was observed among different curing systems whereas this difference is minimized at higher loadings when polymer–filler interaction overshadows the effect of the crosslinking system. Scanning electron microscope studies of tensile fracture surfaces have been made. While filler has marked effect on fracture mode, crosslinking system seems to have little effect. Unfilled (gum) and carbon-black (N 550) filled XNBR vulcanizates show different fracture patterns irrespective of the curing system. This is true in the case of sulphur, metal oxide and metal oxide–sulphur mixed crosslinking systems. But the dicumyl peroxide cured system shows a different fracture pattern and the difference is more in the case of gum vulcanizates.

Keywords Carboxylated nitrile rubber; reinforcement; curing system; polymer–filler interaction; fracture; scanning electron microscopy

INTRODUCTION

In our earlier paper[1] we have reported the effect of crosslinking systems on technical properties of carbon-black-filled carboxylated nitrile rubber (XNBR). Scanning electron microscopy (SEM) studies[2] on failure mechanism of tear have revealed that tear strength of carbon black-filled XNBR vulcanizates varies with the nature of the crosslinking system. Chemical effects of carbon black on sulphur vulcanization have been reviewed by Studebaker[3]. De and coworkers have shown that HAF black filler has catalytic action on vulcanization of natural rubber[4,5]. Voet *et al.*[6] observed that in silica-filled SBR vulcanizate, the extent of reinforcement depends on the type of curing agent used. We have earlier studied the polymer–filler interaction of silica- and clay-filled XNBR system in mixed crosslinking[7] and epoxy-cured systems[8]. These observations have also been extended to epoxy-cured carbon black-filled system[8] and it was found that carbon black filler has no detectable effect on vulcanization of XNBR by epoxy resin.

In the present paper we report results of our studies on the effects of carbon black on vulcanization, polymer–filler interaction, technical properties and fracture mode of XNBR vulcanizates cured by four different crosslinking agents, namely (a) metal oxide, (b) sulphur, (c) dicumyl peroxide and (d) metal oxide–sulphur mixed crosslinking system.

SEM studies have been made to find out the effects of filler and curing systems on the correlation between the technical properties and the tensile fracture topography of carboxylated nitrile rubber.

EXPERIMENTAL

Various mixes were prepared from one stock of XNBR according to the formulations given in *Table 1*. Mixing was done in a conventional laboratory mill at 30°–40°C, according to ASTM D15-70. Mixes were vulcanized at 150°C at their respective optimum cure times as obtained from Monsanto rheometer R-100.

Optimum cure time

In the case of XNBR which shows marching modulus, optimum cure time was calculated as follows: two tangents AC and BC were drawn on the rheograph as shown in *Figure 1*. They meet each other at point C. The points of contact (A and B) of the tangents and rheograph were connected by a straight line AB. The middle point O of the straight line was connected with point C (point of interaction of the two tangents). The line CO cuts the rheograph at point T. The time corresponding to the modulus at point T of the rheograph was taken as the optimum cure time. When this procedure was followed for rheographs showing plateau (i.e. for natural rubber) the time corresponding to the point T is equivalent to the t_{90} value as calculated from the formula,

$$[0.90(L_f - L_i) + L_i]$$

where L_f and L_i are the maximum and minimum rheometric torques.

The details of preparation of vulcanizates and testing procedures are described in an earlier publication[9]. The hysteresis ratio H, defined as the energy dissipated relative to the energy supplied in stretching the specimen, was

0032-3861/83/081055-08$03.00

Table 1 Formulations of the mixes

Mix	A	B	C	D
Krynac 221[a]	95	95	100	100
Stearic acid	2	2	2	2
Krynac PA 50[b]	10	10	–	–
FEF black (N 550)[c]	variable	variable	variable	variable.
Sulphur	–	2.4	2.4	–
CBS[d]	–	0.8	0.8	–
DCP[e]	–	–	–	2

[a] Highly carboxylated nitrile rubber with medium acrylonitrile content. Obtained from Polysar Limited, Ontario, Canada: Mooney number, ML(1 + 4) at 100°C, 50; total ash content, 0.77%; non-staining antioxidant; specific gravity, 0.98
[b] 50/50 technical grade zinc peroxide/NBR masterbatch obtained from Polysar Limited, Ontario, Canada
[c] Carbon black, obtained from Phillips Carbon Black Ltd, Durgapur
[d] *N*-Cyclohexyl benzothiazolesulphenamide, obtained from ACCI Ltd, Rishra
[e] Dicumyl peroxide, obtained from BDH, England

determined[10] from the areas A_1 and A_2 under the loading and unloading force–displacement relations as shown in *Figure 2*. The specimens were stretched to 75% elongation at a rate of elongation of about 0.01 s^{-1} and then allowed to retract at the same rate back to the unstrained state. The mechanical hysteresis was then calculated as follows:

$$H = \frac{A_1 - A_2}{A_1} \quad (1)$$

In the present work, V_r (volume fraction of rubber in the swollen vulcanizate) was determined by assuming that the filler does not swell. Swelling was done in chloroform at 35°C for 36 h when equilibrium was achieved. V_r was calculated as

$$V_r = \frac{(D - FT)\rho_r^{-1}}{(D - FT)\rho_r^{-1} + A_0\rho_s^{-1}} \quad (2)$$

where T is the weight of the test specimen, D the deswollen weight of the test specimen, F the weight fraction of insoluble components of the vulcanizate, A_0 the weight of the absorbed solvent corrected for the swelling increment, ρ_r and ρ_s are the densities of the rubber and solvent respectively ($\rho_r = 0.98$ g cm^{-3} for XNBR and $\rho_s = 1.48$ g cm^{-3} for chloroform).

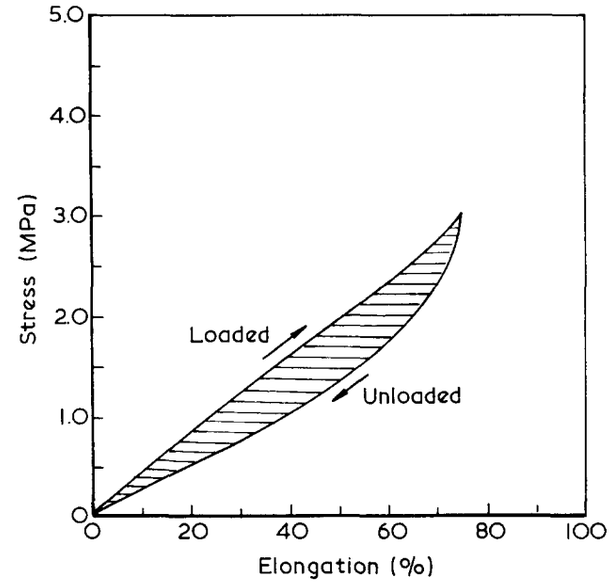

Figure 2 Model stress–strain curve for a deformation cycle[10]

Scanning electron microscope studies

After testing, fracture surfaces were carefully cut from one of the two pieces of the failed test specimen, as illustrated in *Figure 3*, without disturbing the surfaces. The samples were stored in a desiccator to avoid contamination and then sputter-coated with gold within 24 h of testing. SEM observations were made using a Philips 500 model scanning electron microscope. The orientation

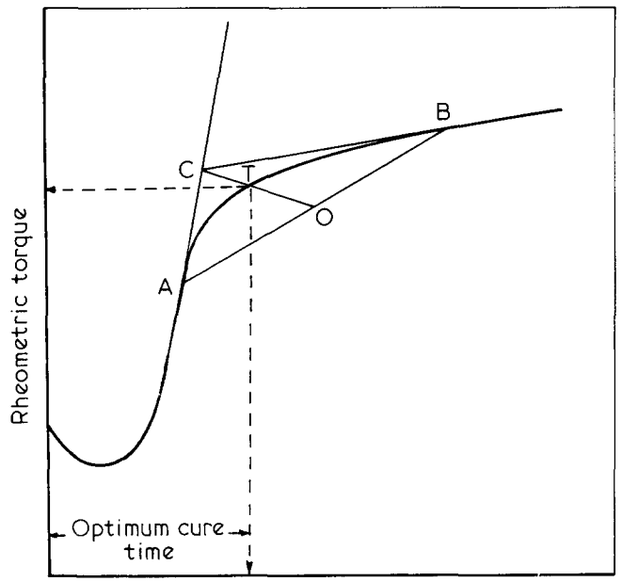

Figure 1 Plot to determine optimum cure time by modified tangent method

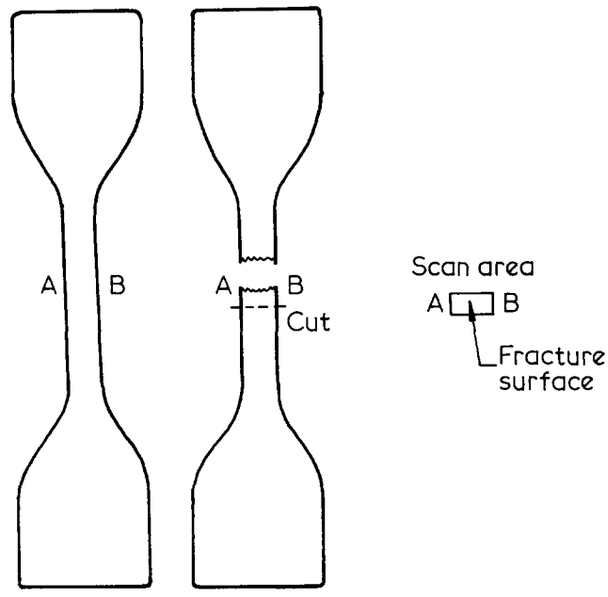

Figure 3 Tensile specimen with fracture direction and direction of photographs

of the photographs was kept the same in all cases. *Figure 11* shows a micrograph taken close to the edge from which fracture started and *Figure 12* is the magnified form of a tear path as also shown in *Figure 11*. In the rest of the cases the failed surface showed uniform characteristics.

RESULTS AND DISCUSSION

Vulcanization studies

Curing characteristics of the mixes as determined by the Mooney viscometer and Monsanto rheometer are recorded in *Table 2*. Increase of carbon black loading decreases the scorch time and optimum cure time and increases the rate of cure. The change of optimum cure time in the case of only sulphur- (mix C) and of only peroxide- (mix D) cured systems is less. Scorchiness of the XNBR mix is due to the metal oxide (Krynac PA 50). Only sulphur or only DCP systems show better scorch safety. Rheographs of different curing systems at varying carbon black loadings are shown in *Figures 4–7*. The maximum and minimum rheometric torques expectedly increase with increase in carbon black loadings, but the extent of increment varies with the curing system used.

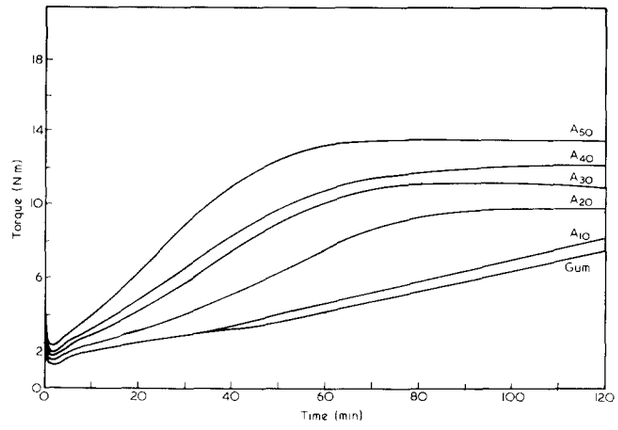

Figure 4 **Rheographs of mix A at varying carbon black loadings at 150°C**

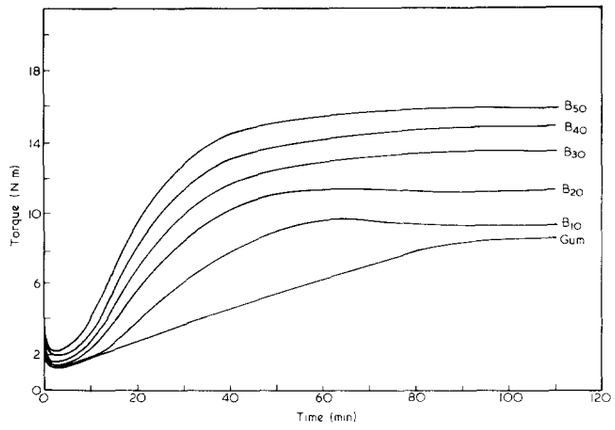

Figure 5 **Rheographs of mix B at varying carbon black loadings at 150°C**

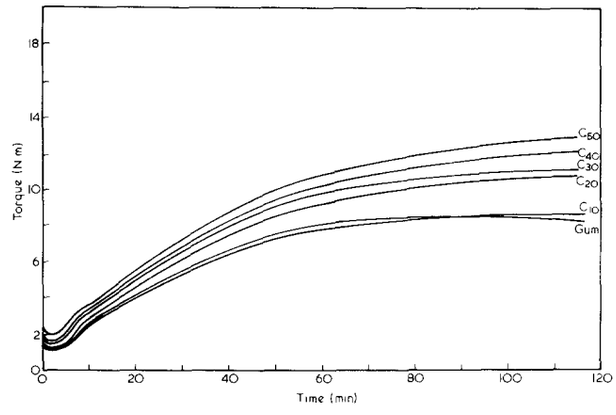

Figure 6 **Rheographs of mix C at varying carbon black loadings at 150°C**

The cure behaviour (Monsanto rheometer) of filled stock cured by different curing agents was examined by modified Westlinning and Wolf equation[11,12]:

$$\frac{\Delta L_f}{\Delta L_g} - 1 = \frac{\alpha_F \phi}{1-\phi} \tag{3}$$

Table 2 Curing characteristics of the mixes using Mooney viscometer and Monsanto rheometer

Mix[a]	A_0	A_{10}	A_{20}	A_{30}	A_{40}	A_{50}	B_0	B_{10}	B_{20}	B_{30}	B_{40}	B_{50}
Mooney scorch time, at 120°C (t_5) (min)	14.0	12.0	11.0	10.5	9.5	8.0	10.0	9.0	8.5	8.0	7.0	6.0
Mooney number, *ML* (1+4)	28	37	42	48	64	74	29	31	37	44	55	66
Optimum cure time, at 150°C (min)	100	80	70	65	52	50	52	45	40	35	33	30
Cure rate (% min^{-1})	0.80	1.30	1.49	1.61	2.10	2.20	2.00	2.45	2.80	3.00	3.40	3.50
Mix[a]	C_0	C_{10}	C_{20}	C_{30}	C_{40}	C_{50}	D_0	D_{10}	D_{20}	D_{30}	D_{40}	D_{50}
Mooney scorch time, at 120°C (t_5) (min)	56.0	45.0	43.0	38.0	34.0	32.0	17.0	15.0	14.0	12.0	11.0	9.0
Mooney number, *ML* (1+4)	29	36	40	45	51	60	22	23	27	31	42	50
Optimum cure time, at 150°C (min)	68	66	63	60	55	57	31	29	26	23	22	21
Cure rate (% min^{-1})	1.60	1.66	1.74	1.82	2.00	2.09	3.45	3.70	4.17	4.65	4.88	5.00

[a] Subscripts indicate the carbon black loading in phr

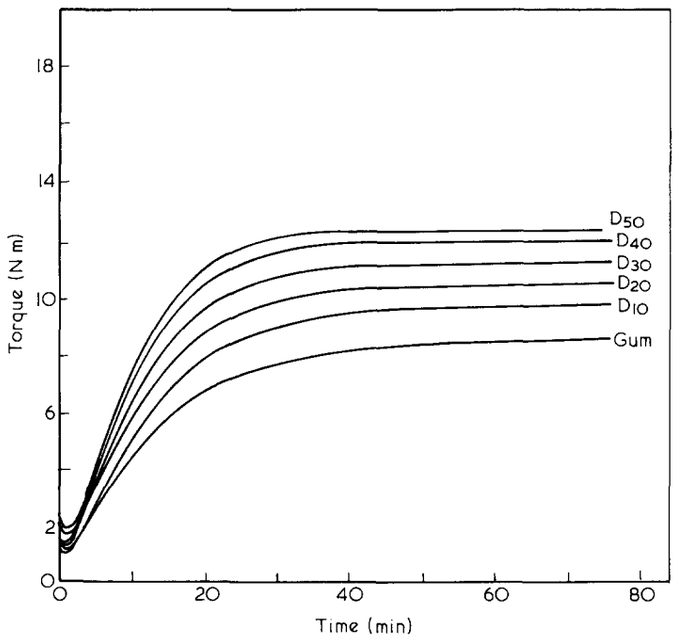

Figure 7 Rheographs of mix D at varying carbon black loadings at 150°C

where ΔL_f and ΔL_g stand for maximum torque, measured with filled and gum stocks respectively, and ϕ is the volume fraction of filler in the filled vulcanizate. *Figure 8* shows the plots of $[\Delta L_f/\Delta L_g - 1]$ vs. $\phi/(1-\phi)$. Variation of the slopes of the straight lines for mix A and mix B indicates that carbon black might have some effects on vulcanization reaction. *Table 3* gives the value of network

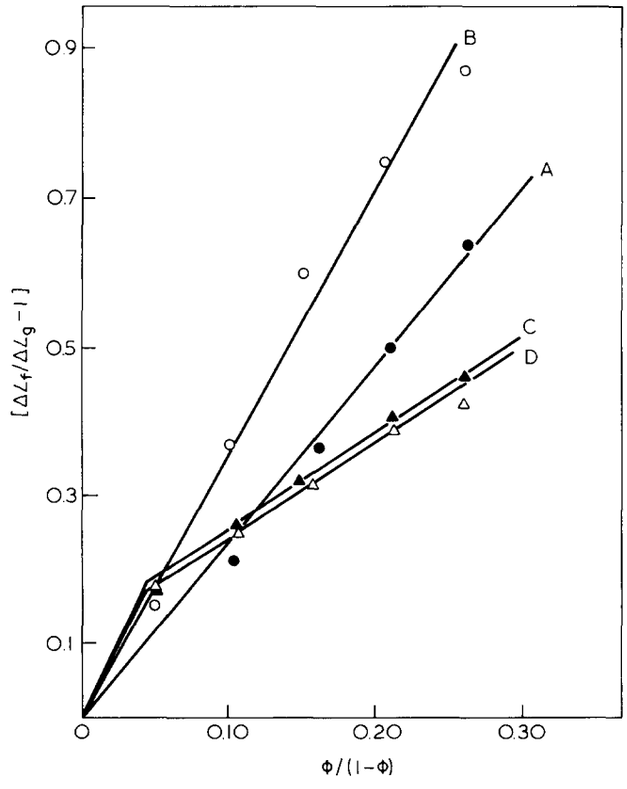

Figure 8 Plots according to Westlinning and Wolf equation[11]

Table 3 Variation of network combined sulphur (S_c) with cure time

Mix	Cure time (min)	Network combined sulphur $(S_c)' \times 10^4$/g RH
B_0	10	1.23
	15	1.40
	20	1.83
	30	3.38
	50	6.47
	100	7.08
B_{40}	10	5.07
	20	7.07
	33	7.08
	45	6.94
	60	6.85
C_0	30	5.29
	50	5.83
	68	6.70
	100	6.91
	120	6.92
C_{40}	30	5.60
	40	5.70
	55	6.80
	70	6.85
	90	6.85

combined sulphur (S_c) cured at different times of metal oxide–sulphur mixed and sulphur-cured gum and filled vulcanizates. The variation of S_c of gum and filled vulcanizates in the mixed curing system (mix B) and constancy of the same in the sulphur-cured system (mix C) support the role of carbon black in vulcanization reaction in the mixed system, as explained earlier by Bhowmick and De[13]. Porter[14] also reported that reinforcing carbon black influences the chemistry of sulphuration of the conventional sulphur vulcanizing system of natural rubber.

The polymer–filler interaction of FEF black-filled XNBR vulcanizates in different curing systems has been studied by the methods of Kraus[15] and Lorenz and Parks[16].

Polymer–filler interaction

According to the Kraus equation[15]

$$\frac{V_{r0}}{V_{fr}} = 1 - m\phi/(1-\phi) \tag{4}$$

where V_{r0} represents the volume fraction of rubber in the unfilled (gum) vulcanizate and V_{rf} is the volume fraction of rubber in the filled vulcanizate. *Figure 9* shows the Kraus plots for XNBR vulcanizates cured by different curing agents. It is evident that carbon black obeys the equation irrespective of curing agent and filler loadings. Polymer–filler interaction follows the pattern,

A(ionic) > B(ionic/S mixed) > C(sulphur) > D(DCP).

The extent of reinforcement was further analysed by the equation of Lorenz and Parks[16]:

$$\frac{Q_f}{Q_g} = ae^{-z} + b \tag{5}$$

or

$$\frac{V_{r0}(1-V_{rf})}{V_{rf}(1-V_{r0})} = ae^{-z} + b \tag{6}$$

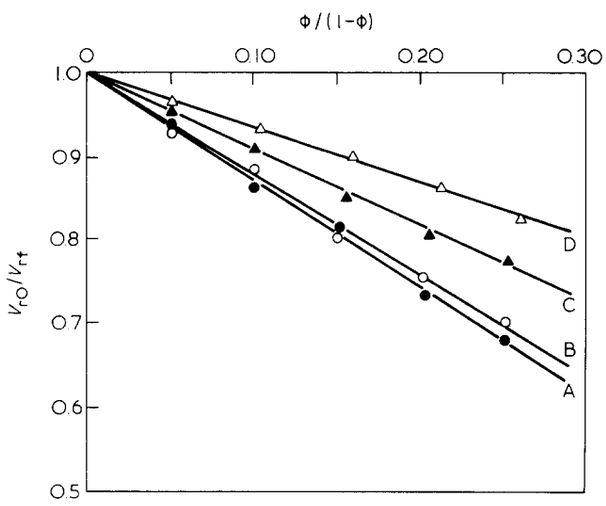

Figure 9 Kraus plots[15]

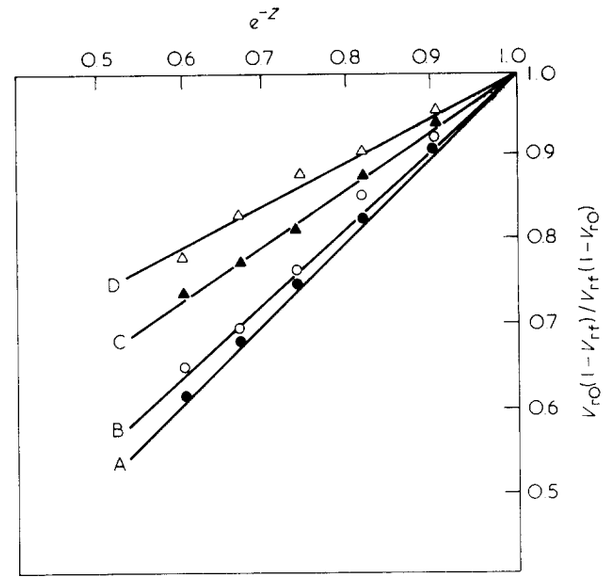

Figure 10 Plots according to Lorenz and Park equation[16]

where Q is the amount of solvent imbibed per unit weight of the rubber, f and g refer to filled and gum mixes and Z is the ratio by weight of filler to rubber vulcanizate. *Figure 10* shows the plots of $V_{r0}(1-V_{rf})/V_{rf}(1-V_{r0})$ vs.e^{-Z} wherein we find that the variation of slopes of the straight lines for different systems follows the same pattern as in the Kraus plots. Physical properties of the XNBR vulcanizates cured by different curing systems at variable black loadings are shown in *Table 4*. Let us first discuss the tensile strength of the gum vulcanizates. Metal-oxide-cured gum vulcanizates show maximum tensile strength. It is believed that tensile strength of gum vulcanizates mainly depends on the stress relaxation (hysteresis loss) and self-reinforcement of the vulcanizates. As the metal-oxide-cured vulcanizates show higher hysteresis (*Table 4a*) and self-reinforcement[17], it shows highest strength in gum vulcanizates. Addition of carbon black enhances tensile strength, modulus, hardness, tear strength and decreases the elongation at break and resilience. At 50 phr carbon black loading all the vulcanizates, irrespective of their curing agents, show almost similar tensile strength. This indicates that at higher filler loading the tensile strength is mainly guided by the slippage of polymer chains over filler surfaces. In the case of mixes C and D, the elongation at break changes very slightly with filler loading, whereas in

Table 4 Physical properties and chemical characterization of the vulcanizates

Property	A_0	A_{10}	A_{20}	A_{30}	A_{40}	A_{50}	B_0	B_{10}	B_{20}	B_{30}	B_{40}	B_{50}
Tensile strength (MPa)	8.84	12.90	16.51	18.71	22.35	21.66	4.49	7.04	16.17	18.61	20.09	20.97
Modulus at 100% elongation (MPa)	1.46	2.49	4.49	6.70	8.24	12.72	1.52	1.60	2.65	4.63	6.87	10.10
Elongation at break (%)	490	320	270	240	230	170	340	360	360	300	225	200
Hardness shore, *A*	65	70	75	80	90	90	65	65	70	80	85	90
Tear strength ($kN\ m^{-1}$)	17.15	28.85	31.46	34.26	36.50	36.67	17.25	26.19	35.78	41.42	46.73	46.46
Resilience (%)	38	36	34	33	32	32	45	41	41	40	35	35
Hysteresis ratio, *H*	0.30	0.15	0.20	0.27	0.31	0.49	0.06	0.12	0.15	0.18	0.22	0.37
Volume fraction of rubber, V_r	0.164	0.175	0.192	0.205	0.225	0.240	0.174	0.182	0.195	0.218	0.231	0.246

Property	C_0	C_{10}	C_{20}	C_{30}	C_{40}	C_{50}	D_0	D_{10}	D_{20}	D_{30}	D_{40}	D_{50}
Tensile strength (MPa)	1.54	8.93	15.50	19.44	20.12	20.47	1.49	4.33	7.49	16.47	18.39	20.87
Modulus at 100% elongation (MPa)	0.60	1.34	1.70	2.54	3.28	4.62	1.17	1.22	1.71	2.06	3.17	4.07
Elongation at break (%)	465	460	460	460	440	380	180	280	300	360	350	340
Hardness shore, *A*	50	55	60	68	74	78	50	55	60	65	70	75
Tear strength ($kN\ m^{-1}$)	12.17	23.75	34.37	43.69	49.10	52.05	7.92	13.80	25.09	30.60	39.40	42.25
Resilience (%)	60	55	50	46	42	40	56	54	53	49	46	43
Hysteresis ratio, *H*	0.05	0.05	0.05	0.08	0.20	0.25	–	–	–	0.09	0.19	0.25
Volume fraction of rubber, V_r	0.159	0.167	0.180	0.189	0.195	0.202	0.162	0.168	0.174	0.180	0.188	0.201

mixes A and B, the decrease of the elongation at break is higher with increase in filler loading. The increase of V_r (volume fraction of rubber) with filler loadings is higher in the case of mixes A and B than for mixes C and D. This is due to tighter network of mixes A and B, which lowers the elongation at break.

Hysteresis ratio of XNBR vulcanizates at varying filler loadings have been studied by static deformation as described earlier. In the gum vulcanizates, mechanical hysteresis follows the order:

ionic > mixed > sulphur > peroxide.

This is also the same order as the polymer–filler interaction. But addition of filler (10 phr carbon black) first decreases the hysteresis of metal-oxide-cured system (mix A) then increases with further addition of carbon black. But in the case of the mixed system (mix B) addition of filler slowly increases the hysteresis up to 40 phr loading, beyond which the increase is abrupt. Only sulphur-cured stock shows very low hysteresis in gum stage and addition of filler increases it rapidly. The DCP-cured system does not show any hysteresis up to 30 phr but beyond 30 phr carbon black loading hysteresis was observed and shows very high hysteresis at 50 phr.

Carbon black loading of 50 phr enhances the apparent crosslink density (V_r) of the vulcanizates of the mixes C and D, which comprises sulphur and DCP systems, to the extent of 25%, whereas in the case of mixes A and B, this enhancement is around 45%. Earlier[3] the increased crosslink density in the filled system was attributed to the increased polymer–filler attachment only. But this increase may also be due to enhancement of covalent crosslinks between polymer chains due to catalytic action of carbon black in the sulphuration process and not merely due to polymer–filler attachment.

Scanning electron microscope studies of tensile fractured surfaces

SEM photomicrographs of tensile fractured gum vulcanizates are shown in *Figures 11–16*. *Figure 11* is the SEM photomicrograph of the peroxide-cured XNBR gum vulcanizate. The surface shows long narrow tear lines emanating from the edge of the specimen. *Figure 12* shows one such tear line at higher magnification, which indicates that the tear moves in a steady path. Although the

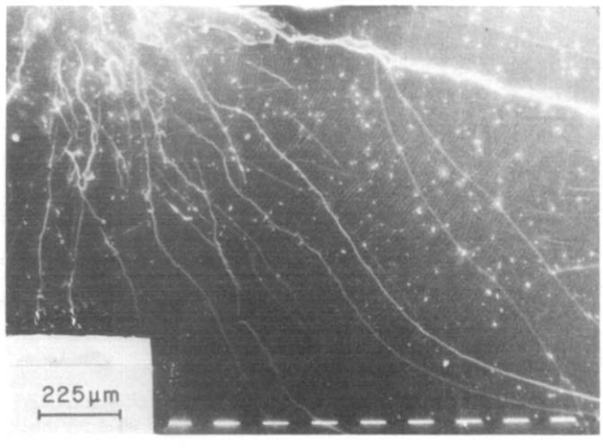

Figure 11 SEM photomicrograph of tensile fracture surface; fine tear lines emanating from edge of mix D (DCP system–gum)

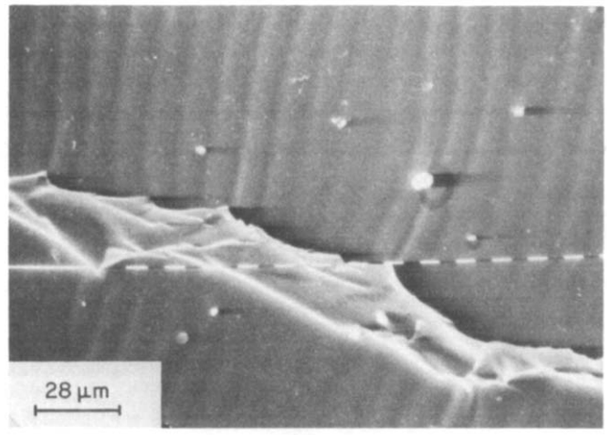

Figure 12 SEM photomicrograph of tensile fracture surface; one tear line of mix D (DCP system–gum) at higher magnification

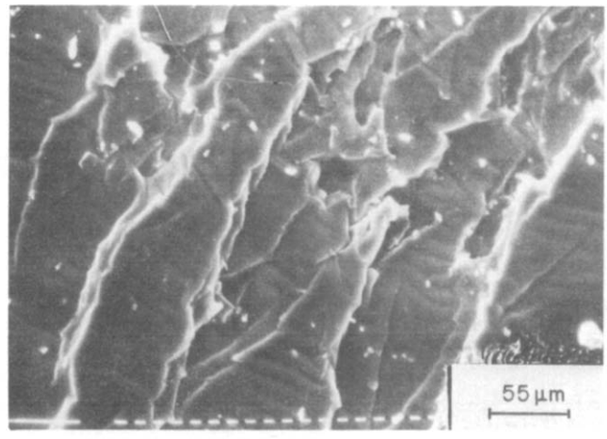

Figure 13 SEM photomicrograph of tensile fracture surface; fracture in different planes with a number of tear lines of mix D (DCP system–gum)

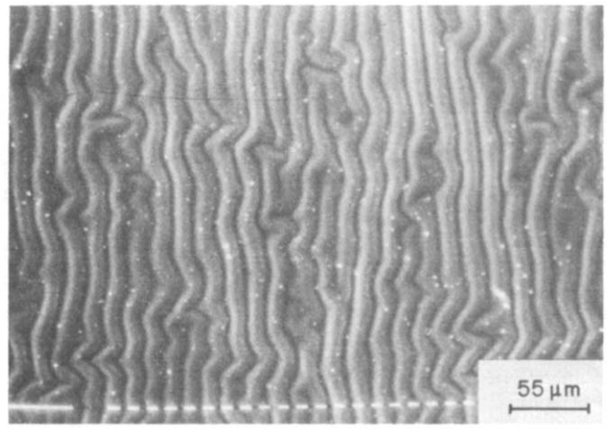

Figure 14 SEM photomicrograph of tensile fracture surface; unidirectional ripplings on the surface of mix A (ionix system–gum)

application of tensile force is considered to be uniform throughout the test specimen, the occurrence of natural flaws and edge nicks in the tensile test specimen, which are quite unavoidable, causes concentration of stress at certain localized points. Failure starts at these points, where the actual stress experienced is much higher than that in the bulk of the specimen. Because of the high stress rupture and the complex stress distribution around the natural flaws, the fracture surface becomes rough at the point of initiation. Once the failure starts, it proceeds as a catastrophic tear giving rise to a layer surface (*Figure 13*) with a number of tear lines. This type of tensile fracture surface has been reported by earlier workers[18-20]. Very feeble ripplings were observed on the surface. But in the case of other vulcanizing systems (sulphur, metal oxide and metal oxide–sulphur mixed system) tensile fracture surfaces of XNBR gum vulcanizates produce different modes of fracture. *Figure 14* shows the tensile fracture surface of metal-oxide-cured gum XNBR (mix A) vulcanizates. Fine ripplings observed on the surface are in one direction (i.e. perpendicular to the direction of fracture propagation) and are regular. In the case of mixed system cured vulcanizates (mix B) similar rippling or microfolding was observed (*Figure 15*). Ripplings are not very regular in this case. Randomness of microfolding is further increased (*Figure 16*) in the case of only sulphur cured system (mix C). A similar observation was made earlier in the case of epoxy-cured gum XNBR vulcanizate[8]. The formation of unidirectional ripplings in the case of mix A (*Figure 14*) is due to better stress dissipation through the ionic crosslinks[1]. The multidirectional microridges in case of mix C (*Figure 16*) indicate many fracture fronts. The distribution of stress at the crack tip of an elastomer depends on the easiness of its propagation. This has been explained by Andrews[21].

Figures 17–20 show the tensile fractured surfaces of the filled XNBR vulcanizate. The addition of carbon black increases the hardness of the vulcanizates, resulting in a very stiff matrix. Addition of carbon black increases the tensile strength remarkably and the mode of stress distribution during tensile testing is different from that in the unfilled vulcanizates. Hence it is obvious that the fractured surfaces of the tensile specimen will be different if the fracture surface is correlated with the strength property. A SEM photomicrograph of tensile fractured DCP-cured filled vulcanizate is shown in *Figure 17*. The whole surface appears rough with a large number of curved tear lines. This type of rough fracture surface in the case of

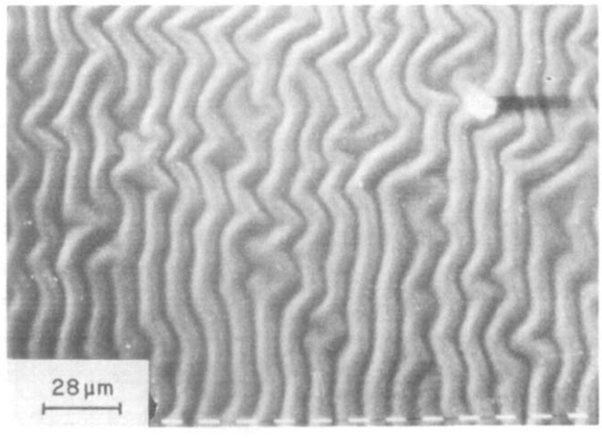

Figure 15 SEM photomicrograph of tensile fracture surface; multidirectional ripplings of mix B (ionic/S mixed system–gum)

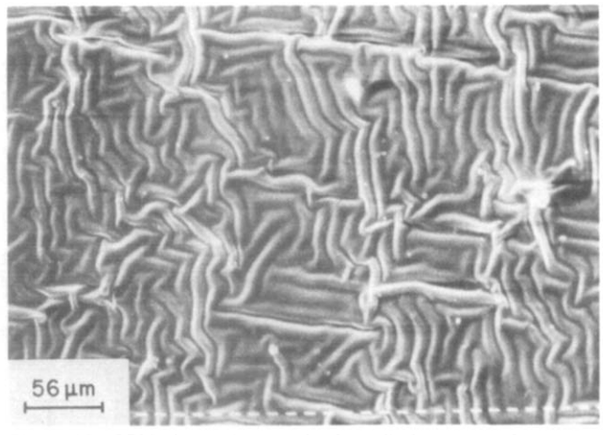

Figure 16 SEM photomicrograph of tensile fracture surface; ripplings in random direction of mix C (sulphur system–gum)

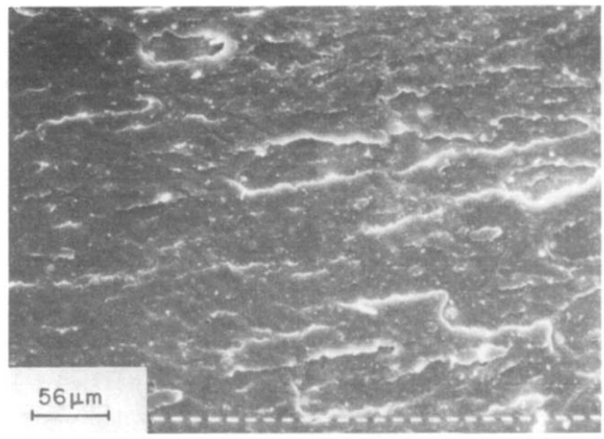

Figure 17 SEM photomicrograph of tensile fracture surface: rough surface with curved tear lines of mix D (DCP system – 40 phr FEF black filled)

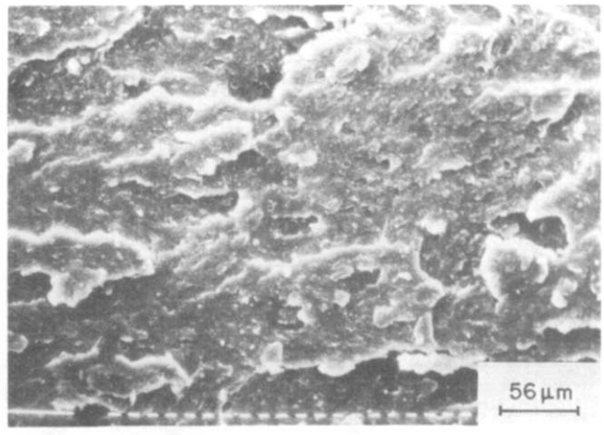

Figure 18 SEM photomicrograph of tensile fracture surface; rough surface of mix C (sulphur system – 40 phr FEF black filled)

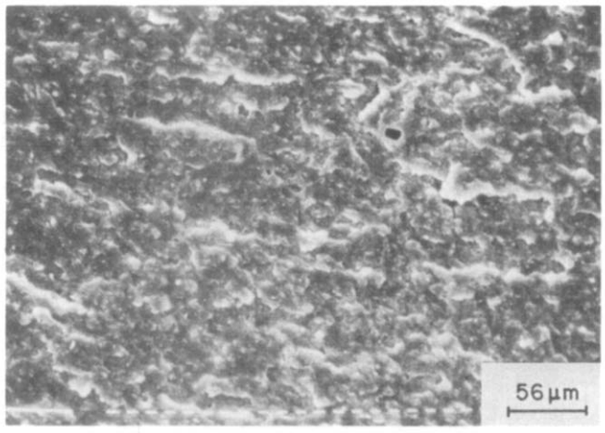

Figure 19 SEM photomicrograph of tensile fracture surface; more rough surface of mix B (ionic/S mixed system – 40 phr FEF black filled)

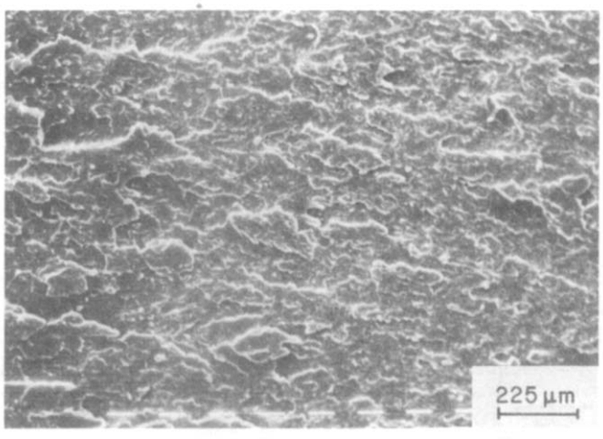

Figure 20 SEM photomicrograph of tensile fracture surface; rugged surface of mix A (ionic system – 40 phr FEF black filled)

carbon-black-filled natural rubber vulcanizates has been reported earlier[8,18–20]. Tensile fracture surface (*Figure 18*) of only sulphur cured XNBR filled vulcanizate shows more rough surface. The metal oxide–sulphur mixed system shows a similar pattern (*Figure 19*). As the roughness of the surface increases, the strength of the vulcanizates increases. This indicates that the fracture propagation has occurred in more than one plane. This is also clear in the case of only metal oxide cured fracture surface (*Figure 20*). The general fracture pattern of filled vulcanizates is almost the same irrespective of the vulcanizing system.

REFERENCES

1 Chakraborty, S. K., Bhowmick, A. K. and De, S. K. *J. Appl. Polym. Sci.* 1981, **26**, 4011
2 Chakraborty, S. K., Bhowmick, A. K., Dhindaw, B. K. and De, S. K. *Rubber Chem. Technol.* 1982, **55**, 41
3 Studebaker, M. L. *Rubber Chem. Technol.* 1957, **30**, 1070
4 Bhowmick, A. K. and De, S. K. *Rubber Chem. Technol.* 1980, **53**, 1015
5 Pal, P. K., Bhowmick, A. K. and De, S. K. *Rubber Chem. Technol.* 1982, **55**, 23
6 Voet, A., Morawski, J. C. and Donnet, J. B. *Rubber Chem. Technol.* 1977, **50**, 342
7 Chakraborty, S. K. and De, S. K. *Rubber Chem. Technol.* 1982, **55**, 990
8 Chakraborty, S. K. and De, S. K. *J. Appl. Polym. Sci.* 1982, **27**, 4561
9 Mukhopadhyay, R., De, S. K. and Chakraborty, S. N. *Polymer* 1977, **18**, 1243
10 Dreyfuss, P., Gent, A. N. and Williams, J. R. *J. Polym. Sci., Polym. Phys. Edn.* 1980, **18**, 2135
11 Westlinning, H. and Wolf, S. *Kautsch. Gummi Kunstst.* 1966, **19**, 470; 1970, **23**, 7
12 Cotten, C. R. *Rubber Chem. Technol.* 1972, **45**, 129
13 Bhowmick, A. K. and De, S. K. *J. Appl. Polym. Sci.* 1980, **26**, 529
14 Porter, M. *Rubber Chem. Technol.* 1967, **40**, 866
15 Kraus, G. *J. Appl. Polym. Sci.* 1963, **7**, 861; *Rubber Chem. Technol.* 1964, **37**, 6
16 Lorenz, O. and Parks, C. R. *J. Polym. Sci.* 1961, **50**, 299
17 Brown, H. P. *Rubber Chem. Technol.* 1963, **36**, 931
18 Bascom, W. D. *Rubber Chem. Technol.* 1977, **50**, 875
19 Mathew, N. M. and De, S. K. *Polymer* 1982, **23**, 632
20 Mathew, N. M., Bhowmick, A. K., Dhindaw, B. K. and De, S. K. *J. Mater. Sci.* 1982, **17**, 2594
21 Andrews, E. H. *J. Appl. Phys.* 1961, **32**(3), 542